The Journal of Nutrition
Ingestive Behavior and Neurosciences

High Dietary Iron Has a Greater Impact on Brain Iron Homeostasis and Cognitive Function in Old Compared with Young C57BL/6J Male Mice

Min Chen,[1,2] En Xu,[2,3] Chong Zeng,[2] Wenjie Zhu,[4] Jiashuo Zheng,[2,5] and Huijun Chen[2]

[1]Clinic for Psychiatry and Psychotherapy, Ludwig-Maximilians-Universität München, München, Germany; [2]Jiangsu Key Laboratory of Molecular Medicine, Medical School of Nanjing University, Nanjing, China; [3]Department of General Surgery, Affiliated Drum Tower Hospital, Medical School of Nanjing University, Nanjing, China; [4]Department of Urology, Nanjing Drum Tower Hospital, The Affiliated Hospital of Nanjing University Medical School, Institute of Urology, Nanjing University, Nanjing, China; and [5]Helmholtz Zentrum München, Institute of Metabolism and Cell Death, Neuherberg, Germany

ABSTRACT

Background: Brain iron accumulation is a feature of Alzheimer disease (AD) but whether a chronic dietary iron overload contributes to AD induction is unknown. We previously showed that young mice fed a high iron diet did not display cognitive impairment despite the AD pathological markers in hippocampus.

Objectives: We aim to compare the impact of high dietary iron on brain pathologic changes and cognitive function in young and old mice.

Methods: Male C57BL/6J mice at 1 mo and 13 mo of age were fed with either a control diet (66 mg Fe/kg; Young-Ctrl and Old-Ctrl) or a high iron diet (14 g Fe/kg; Young-High Fe and Old-High Fe) for 7 mo, and outcomes were evaluated at 8 mo and 20 mo of age. Iron concentrations in brain regions were measured by atomic absorption spectrophotometry. Perls's Prussian blue staining and amyloid-β (Aβ) immunostaining were performed. Protein expression in the cerebral cortex and hippocampus was determined by immunoblotting. Superoxide dismutase activity and malondialdehyde concentration were examined. Cognitive functions were tested with the Morris water maze system. Two-factor ANOVA was used to analyze most data.

Results: Compared with Old-Ctrl mice, Old-High Fe mice showed significantly higher iron concentrations in cerebral cortex (60% higher), cerebellum (60% higher), and hippocampus (90% higher), paralleled by lower superoxide dismutase activity and greater malondialdehyde concentration in cerebral cortex and hippocampus and worse cognitive function. In contrast, these variables did not significantly differ between the 2 young groups. Nevertheless, ferritin, phospho-tau, and Aβ_{1-42} expression in hippocampus and ferritin and Aβ_{1-42} expression in cerebral cortex were induced by the high iron diet irrespective of the age of mice (40–200% greater).

Conclusions: High dietary iron induced cognitive defects in old mice but not young mice, suggesting that elderly people should avoid consuming abnormally high concentrations of iron. *J Nutr* 2021;00:1–8.

Keywords: Alzheimer disease, aging, cognitive function, dietary iron overload, oxidative stress

Introduction

Iron is an essential trace element required for many basic physiologic processes in the central nervous system (CNS), but it can also be toxic when present in excess (1). Although body iron concentration is predominantly controlled at the point of absorption in the small intestine and thus could be easily affected by the amount of dietary iron (2), the CNS is also protected by the blood–brain barrier (BBB), which prevents the direct uptake of iron from the systemic circulation.

Nevertheless, brain iron accumulation occurs in both the normal aging process and a range of neurodegenerative diseases, including Alzheimer disease (AD) (1). Since the first report of the association between iron and AD in 1953 (3), postmortem and MRI studies have repeatedly demonstrated that iron deposition in specific brain regions such as cerebral cortex and hippocampus is a key feature of AD (4–8). Despite all these studies, whether iron overload is a primary cause or secondary consequence of AD is still under debate. On the one hand, mouse models of AD and tauopathy both display increased

Manuscript received January 27, 2021. Initial review completed February 25, 2021. Revision accepted May 18, 2021.
First published online 0, 2021; doi: https://doi.org/10.1093/jn/nxab189.

brain iron concentration (9, 10). On the other hand, multiple studies have indicated that iron contributes to the development of AD by promoting the generation of AD pathologic markers amyloid-β (Aβ) and phospho-tau (p-tau) and oxidative stress (8, 11, 12). Our previous work indicated that mice with combined genetic mutations of 2 multicopper ferroxidases, hephaestin and ceruloplasmin, had brain iron accumulation at 6 mo of age, and this was paralleled by oxidative damage and learning and memory defects (13). However, whether dietary iron can directly contribute to the induction of AD is still enigmatic.

To address this question, we previously fed C57BL/6J mice and amyloid precursor protein/presenilin 1 (APP/PS1) double transgenic mice a high iron diet (14 g Fe/kg) from 10 to 30 wk of age to observe the impact of high dietary iron on brain pathologic changes and cognitive function (14). Despite the induction of ferritin, Aβ, and p-tau expression in the hippocampus, the high iron diet did not significantly affect the brain iron concentration and had little impact on oxidative stress or cognitive functions in both mouse strains (14). These results revealed that even though the iron concentration in the plasma was increased by 2- to 3-fold, the changes in brain iron homeostasis could still be subtle.

Considering that neurodegeneration diseases usually occur in elderly people and that the effect of dietary iron on brain might be age dependent, in the present study, we started the iron treatment on C57BL/6J mice at the age of 13 mo, comparable to ~45-y-old human beings, and ended the experiments at the age of 20 mo, comparable to ~60-y-old human beings (15). C57BL/6J mice at a younger age (1–8 mo) were used as a control. We hypothesized that dietary iron overload might have more significant impacts on brain iron contents, pathologic changes, and cognitive function when the mice were at an older age.

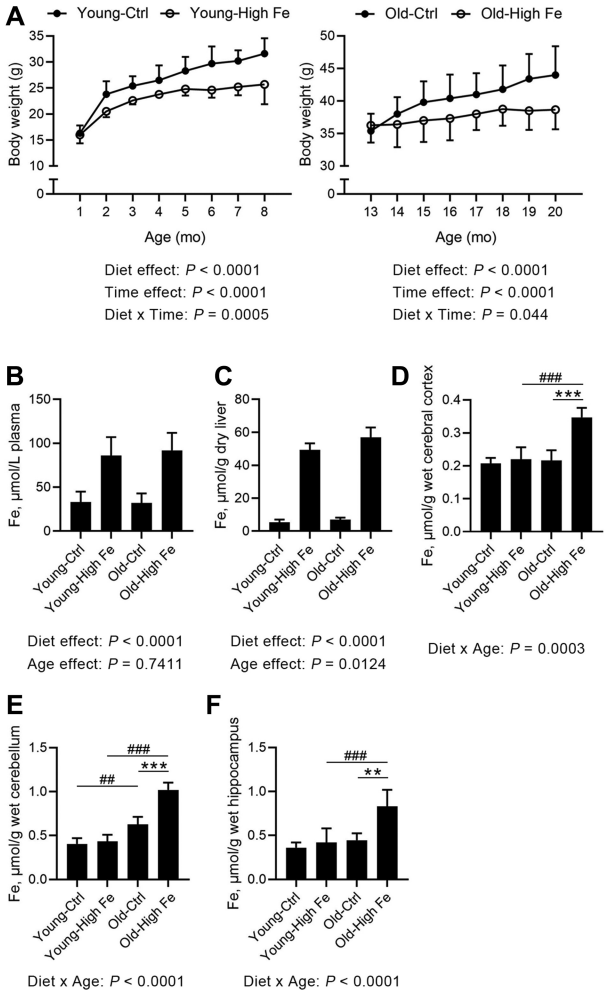

FIGURE 1 Body weight (A) and iron concentrations in the plasma (B), liver (C), cerebral cortex (D), cerebellum (E), and hippocampus (F) of male C57BL/6J mice fed control or high iron diet for 7 mo beginning at 1 mo or 13 mo of age. Values are means ± SDs, $n = 7$ (B–F) or $n = 20$ (A). The P value of the interaction is presented when it reaches significance, and further analysis of diet simple effects and age simple effects was then performed. $^{**}P < 0.01$, $^{***}P < 0.001$, different due to diet; $^{\#\#}P < 0.01$, $^{\#\#\#}P < 0.001$, different due to age.

Methods

Mouse models and dietary treatments

Three-week-old and 12-mo-old C57BL/6J male mice purchased from the Mutant Mouse Regional Resource Center were maintained at the Medical School of Nanjing University until the age of 1 mo and 13 mo, respectively, with unlimited access to AIN-93M control diet (16). Mice then were randomly assigned to a control diet group (Young-Ctrl and Old-Ctrl) or a high iron diet group (Young-High Fe and Old-High Fe), where they were fed with either the AIN-93M control diet or an iron-loaded diet (based on AIN-93M) supplemented with carbonyl iron (14) for 7 mo (i.e., until the age of 8 mo and 20 mo, respectively). The iron concentrations of the control diet and the iron-loaded diet, as measured by atomic absorption spectrophotometry, were 1.18 ± 0.01 μmol/g (~66 mg/kg) and 251 ± 13.36 μmol/g (~14 g/kg), respectively (14). In total, 120 mice were used with 30 mice in each group. The mice were allowed unlimited access to their diets and distilled water. All studies were carried out in accordance with NIH guidelines and approved by the Institutional Animal Care and Use Committee of Nanjing University.

Tissue preparation

Mice were killed at 8 mo and 20 mo of age. Blood was collected by cardiac puncture, and the body was perfused with PBS via the heart. Whole blood was centrifuged to provide plasma. Liver tissues were removed and dried by heating at 80–100°C for 2 h for subsequent iron analysis. Brain tissues were quickly placed on ice and dissected to separate the cerebral cortex, cerebellum, and hippocampus. Brain sections were snap-frozen in liquid nitrogen and then stored at −80°C until they were required for iron concentration or protein analyses. In addition, 4 mice of each group were perfused via the heart, first with PBS and then with 4% paraformaldehyde. The collected brain tissues were fixed in 4% paraformaldehyde solution for later histologic analysis.

Measurement of iron concentrations

Plasma, dried liver tissue, and wet brain sections of cerebral cortex, cerebellum, and hippocampus were digested in nitric acid at 80°C for 2 h

Supported by the National Natural Science Foundation of China grants (81773417 and 81273068) to HC.
Author disclosures: The authors report no conflicts of interest.
MC and EX contributed equally to the article.
Address correspondence to HC (e-mail: hjchen@nju.edu.cn).
Abbreviations used: Aβ, amyloid-β; AD, Alzheimer disease; APP/PS1, amyloid precursor protein/presenilin 1; BBB, blood–brain barrier; CNS, central nervous system; DAB, diaminobenzidine; DG, dentate gyrus; MDA, malondialdehyde; Old-Ctrl, mice fed a control diet from 13 to 20 mo of age; Old-High Fe, mice fed a high iron diet from 13 to 20 mo of age; PBST, Tween-20 in PBS; p-tau, phospho-tau; SOD, superoxide dismutase; Young-Ctrl, mice fed a control diet from 1 to 8 mo of age; Young-High Fe, mice fed a high iron diet from 1 to 8 mo of age.

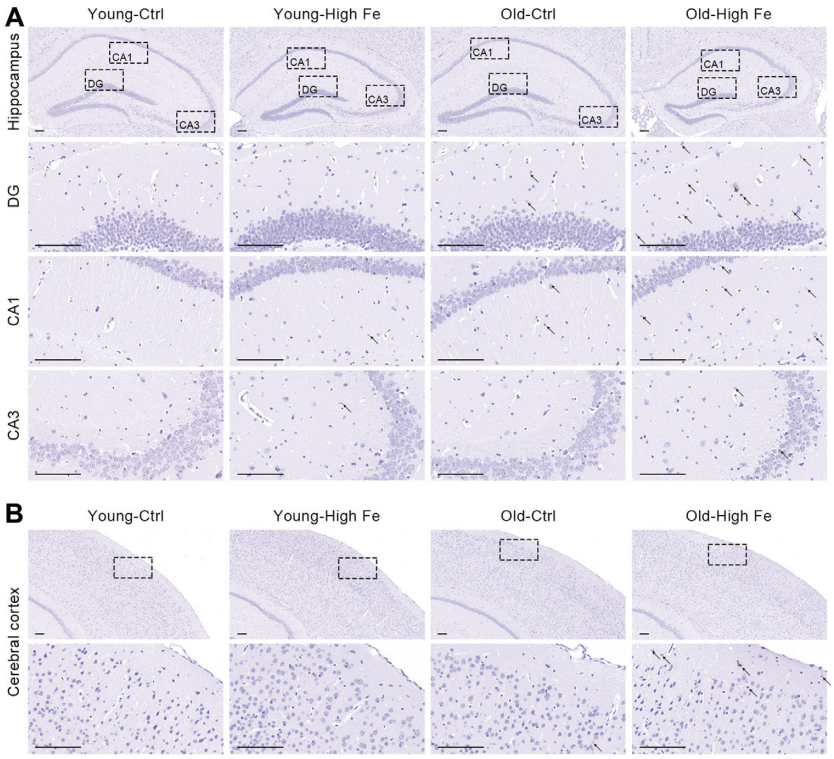

FIGURE 2 Representative images of diaminobenzidine-enhanced Perls's staining for iron (arrows) in the hippocampus (A) and cerebral cortex (B) of male C57BL/6J mice fed control or high iron diet for 7 mo beginning at 1 mo or 13 mo of age, $n = 4$. The images in the lower rows are magnified images of the corresponding regions indicated in the images in the top rows. Bar = 100 μm. DG, dentate gyrus.

and then heated at 100°C for 24 h. Iron concentrations of mouse plasma and tissues were measured using an atomic absorption spectrometer (model 180–80; Hitachi) at the Modern Instrumental Analysis Center of Nanjing University (17). Iron (III) nitrate solution was used as reference standards.

Histology

For diaminobenzidine (DAB)–enhanced Perls's Prussian blue staining (for iron detection), deparaffinized brain sections were stained with 4% hydrochloric acid and 4% potassium ferrocyanide, followed by a series of incubations with DAB staining as previously described (18). Finally, the sections were counterstained with hematoxylin.

For Aβ staining, deparaffinized brain sections were incubated with citrate antigen retrieval solution (pH 6.0, cat. no. G1202; Servicebio) at 95°C for 15 min. Then, sections were allowed to cool slowly, washed in distilled water, and incubated in 3% H_2O_2 for 25 min. Subsequently, sections were blocked in blocking buffer containing 3% BSA and 0.1% Tween-20 in PBS (PBST) at room temperature for 30 min and stained with anti-Aβ antibody (1:100, cat. no. ab2539; Abcam) overnight at 4°C. The next day, sections were washed 3 times with PBST and then incubated with a horseradish peroxidase–labeled goat anti-rabbit secondary antibody (1:200, cat. no. GB23303; Servicebio) for 50 min at room temperature. After extensive washing with PBST 3 times, the sections were washed for 5 min in PBS and incubated with DAB substrate to visualize the antibody. Finally, the sections were counterstained with hematoxylin.

Immunoblot analysis

Cerebral cortex and hippocampus samples ($n = 4$–6 per group) were homogenized in lysing buffer [1× PBS containing 1% Triton X-100, 0.1% SDS, and a protease inhibitor cocktail (cat. no. 539134; Calbiochem)]. For p-tau immunoblots, the lysing buffer was supplemented with 2% alkaline phosphatase inhibitors (cat. no. P1081; Beyotime Biotechnology). The total protein concentration was determined by the bicinchoninic acid method (Bioworld Technology, Inc.), and 35-μg proteins were loaded in each lane. Immunoblot and quantification were performed as previously described (14). The following antibodies were used: anti–ferritin light chain (1:1000; cat. no. sc-74513; Santa Cruz Biotechnology), anti–p-tau (Ser404) (1:1000; cat. no. 44-758G; Invitrogen), anti-A$\beta_{1–42}$ (1:1000; cat. no. ab10148; Abcam), anti–β-tubulin (1:5000; cat. no. M20005; Abmart), anti-mouse secondary antibody (1:2000; cat. no. sc-2031; Santa Cruz Biotechnology), and anti-rabbit secondary antibody (1:40000; cat. no. sc-2030; Santa Cruz Biotechnology).

Superoxide dismutase and malondialdehyde concentration assay

Cerebral cortex and hippocampus samples ($n = 4$–5 per group) were homogenized in PBS and centrifuged at 10,000 × g for 15 min at 4°C. The determination of superoxide dismutase (SOD) activity and malondialdehyde (MDA) concentration was made spectrophotometrically with SOD and MDA assay kits according to the manufacturer's instructions (cat. nos. S0101 and S0131; Beyotime Biotechnology) (13). The measurements of SOD and MDA were based on the WST-8 method and the reaction of MDA and thiobarbituric acid, respectively. To prevent the generation of MDA during tissue processing, antioxidants were added following the manufacturer's instructions for the MDA assay kit. Data were collected using a microplate reader.

Morris water maze

Learning and memory of mice at 7 or 19 mo of age were tested with the Morris water maze system according to the protocol we previously used (14). The Morris water maze system fits into a 1.2-m-diameter circular pool with opaque water (22–24°C). The Morris water maze task was performed similar to that described by Konopka et al. (19) with minor modifications. Briefly, the experiment was divided into 2 phases. For the first 4 d, mice were trained to locate the platform submerged below the water surface. Mice that failed to locate the platform within 90 s were guided to it, with the escape latency recorded

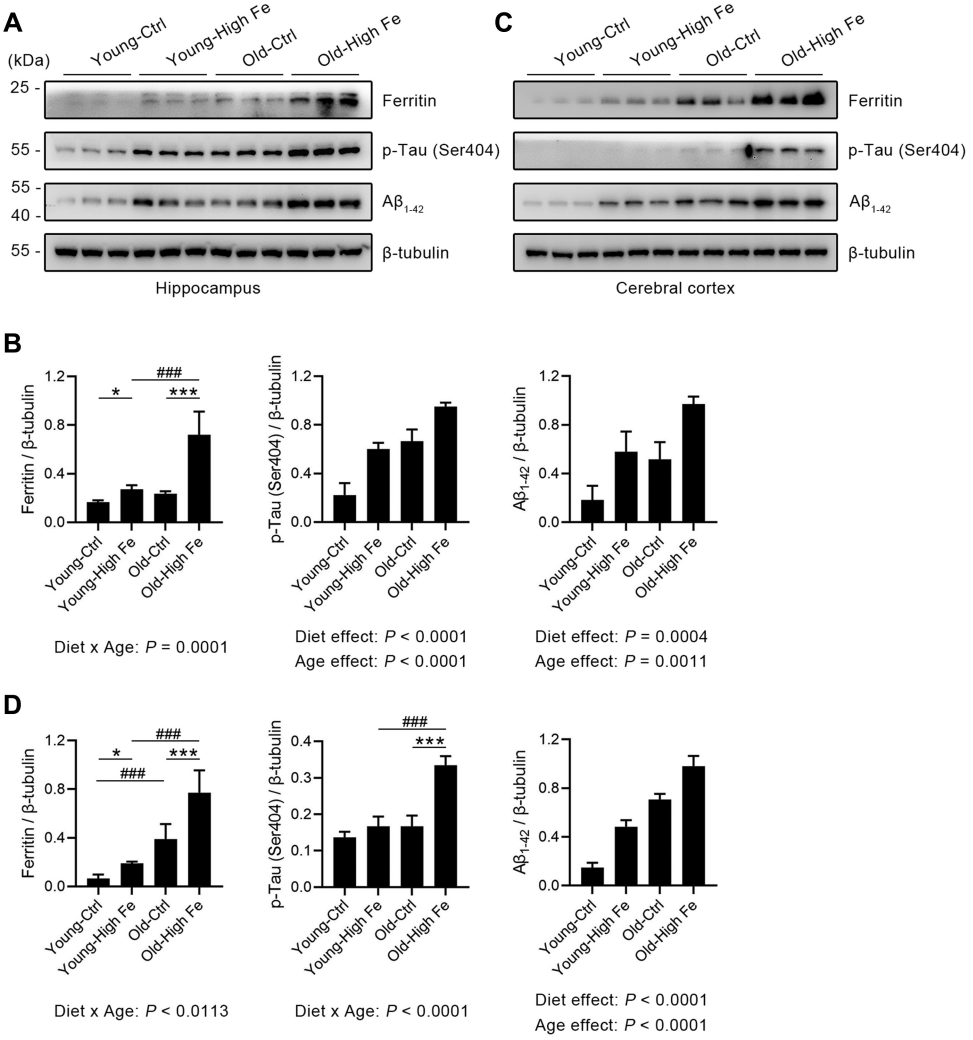

FIGURE 3 Ferritin, p-tau (Ser404), and A$\beta_{1–42}$ protein concentrations in the hippocampus (A) and cerebral cortex (C) of male C57BL/6J mice fed control or high iron diet for 7 mo beginning at 1 mo or 13 mo of age. The immunoblot signals in the hippocampus (B) and cerebral cortex (D) were quantified, and values were normalized using β-tubulin expression. Values are means ± SDs, $n = 6$. The P value of the interaction is presented when it reaches significance, and further analysis of diet simple effects and age simple effects was then performed. $^{*}P < 0.05$, $^{***}P < 0.001$, different due to diet; $^{\#\#\#}P < 0.001$, different due to age. A$\beta_{1–42}$, amyloid-β1–42; p-tau, phospho-tau.

as 90 s. On day 5, a probe test that lasted for 90 s was conducted with the platform removed. Mice were released from the point opposite to the target quadrant, and time to reach the center of the target quadrant where the platform had previously been located was recorded as the escape latency. Swimming velocity, the number of times that each mouse crossed the center of the target quadrant, and the time that each mouse spent in the target quadrant were monitored by a video camera linked to a MiniSee (ScopeTek) computerized tracking system.

Statistical analysis

All values are presented as means ± SDs. Two-factor ANOVA was used to compare plasma and tissue iron concentrations, ferritin, p-tau (Ser404), and A$\beta_{1–42}$ protein concentrations, SOD activity and MDA concentration, and most of the data obtained from the behavioral study. Body weight and escape latency data were analyzed by 2-factor and 3-factor repeated-measures ANOVA, respectively. The P values for main effects or interactions are presented within the relevant figures. Two-factor ANOVA tests with a significant interaction between the 2 factors were further analyzed by Bonferroni post hoc test. Differences were considered significant at $P < 0.05$. All statistical analyses were performed using GraphPad Prism 9 (GraphPad Software).

Results

Weight and iron status of the 4 groups of mice

For both age groups, iron treatment induced significantly lower body weight ($P < 0.0001$) and higher iron concentrations in plasma (~2-fold higher, $P < 0.0001$) and liver (~8-fold higher, $P < 0.0001$) (Figure 1A–C). For mice fed the same diet, age did not significantly affect the plasma iron, but older mice had a significantly higher liver iron concentration than younger mice (~30% higher, $P = 0.0124$). Interestingly, in cerebral cortex, cerebellum, and hippocampus, there were interactions between dietary iron and age. Old-High Fe mice had significantly higher iron concentrations in all these 3 tissues than Young-High Fe mice and Old-Ctrl mice (60–100% higher, $P < 0.01$). In addition, Old-Ctrl mice had a significantly higher iron concentration than Young-Ctrl mice in cerebellum (60% higher, $P < 0.01$) (Figure 1D–F).

Iron accumulates in the hippocampus and cerebral cortex of Old-High Fe mice

Iron distributions in the hippocampus and cerebral cortex were then assessed. Although no visible iron accumulation was

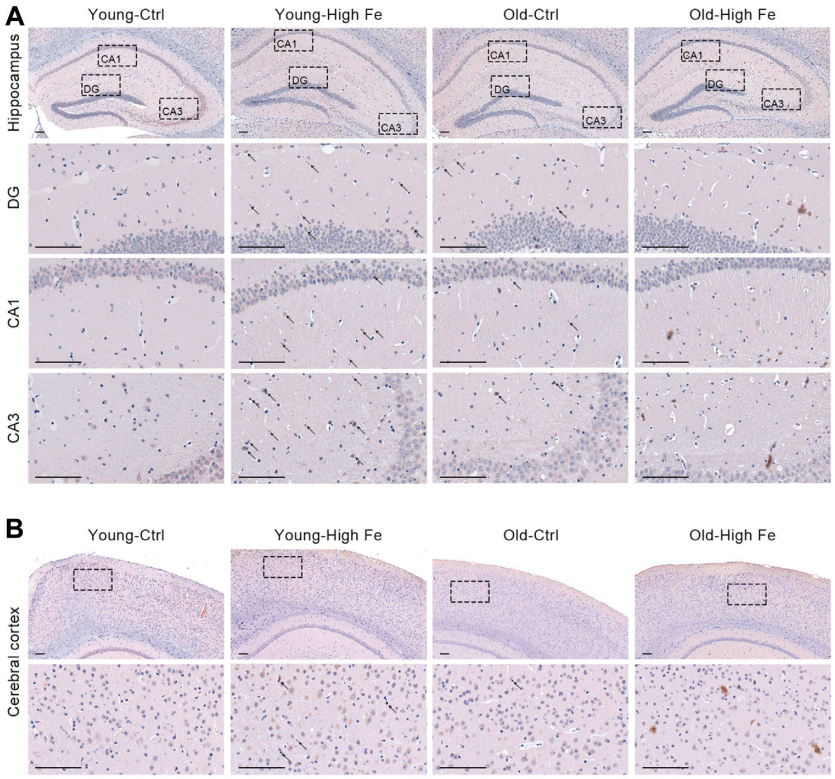

FIGURE 4 Representative images of amyloid-β (Aβ) staining in the hippocampus (A) and cerebral cortex (B) of male C57BL/6J mice fed control or high iron diet for 7 mo beginning at 1 mo or 13 mo of age, $n = 4$. The images in the lower rows are magnified images of the corresponding regions indicated in the images in the top rows. Bar = 100 μm. Aβ spots in the hippocampus and cerebral cortex of Young-High Fe mice and Old-Ctrl mice are indicated with arrows. Bar = 100 μm. DG, dentate gyrus.

detected in Young-Ctrl mice, a small amount of stainable iron was observed in the hippocampal CA1 and CA3 regions of Young-High Fe mice, as well as hippocampal dentate gyrus (DG) and CA1 regions and cerebral cortex of Old-Ctrl mice. In contrast, Old-High Fe mice had multiple iron deposits in the hippocampal DG and CA1 regions as well as the cerebral cortex. A few iron spots were also detected in the hippocampal CA3 region of Old-High Fe mice (**Figure 2**A and B).

Iron treatment induces ferritin, p-tau, and A$\beta_{1–42}$ protein concentrations in the hippocampus and cerebral cortex

Ferritin, p-tau, and A$\beta_{1–42}$ protein concentrations in the hippocampus and cerebral cortex were examined. In hippocampus, there was an interaction between dietary iron and age in ferritin concentration. Young-High Fe mice had a significantly greater ferritin concentration than Young-Ctrl mice (60% greater, $P < 0.05$), and this effect was exacerbated in Old-High Fe mice relative to Old-Ctrl mice (2-fold greater, $P < 0.001$). In addition, the ferritin concentration in Old-High Fe mice was 170% greater than that of Young-High Fe mice ($P < 0.001$). Protein concentrations of p-tau (phosphorylated at Ser404) and A$\beta_{1–42}$ in hippocampus were significantly increased by iron loading ($P < 0.0001$ and $P = 0.0004$, respectively) and age ($P < 0.0001$ and $P = 0.0011$, respectively), but there was no interaction between the 2 factors (**Figure 3**A and B). In cerebral cortex, there was also an interaction between dietary iron and age in ferritin concentration. The ferritin concentration in Old-Ctrl mice was 5-fold greater than that of Young-Ctrl mice ($P < 0.001$), and iron loading tripled and doubled the ferritin concentrations in young age ($P < 0.05$) and old age ($P < 0.001$) groups, respectively. An interaction between dietary iron and age was also found in p-tau concentration. The p-tau concentration in Old-High Fe mice was 1-fold greater than that of Young-High Fe mice and Old-Ctrl mice (both $P < 0.001$). Furthermore, the A$\beta_{1–42}$ protein concentration in cerebral cortex showed a similar pattern to hippocampus, being significantly increased by iron treatment and age (both $P < 0.0001$) (Figure 3C and D).

Iron treatment enhances Aβ deposition in the hippocampus and cerebral cortex

Consistent with our previous report (14), diffusely distributed Aβ spots were observed throughout the whole hippocampus of Young-High Fe mice, whereas there were no Aβ deposits in the hippocampus of Young-Ctrl mice. At 20 mo of age, mice fed a control diet also showed a number of Aβ spots throughout the whole hippocampus, albeit fewer than in Young-High Fe mice. In stark contrast, Old-High Fe mice had numerous Aβ plaques, which were distributed among the hippocampal DG, CA1, and CA3 regions (**Figure 4**A). The pattern of Aβ deposits in cerebral cortex was basically the same as in hippocampus among the 4 groups of mice (Figure 4B).

Old-High Fe mice had oxidative damage in the hippocampus and cerebral cortex

Oxidative stress in hippocampus and cerebral cortex was evaluated by measuring SOD activity and MDA concentration. In hippocampus, there were interactions between dietary iron and age in both SOD activity and MDA concentration (**Figure 5**A). Old-High Fe mice had significantly lower SOD activity and greater MDA concentration than Young-High Fe

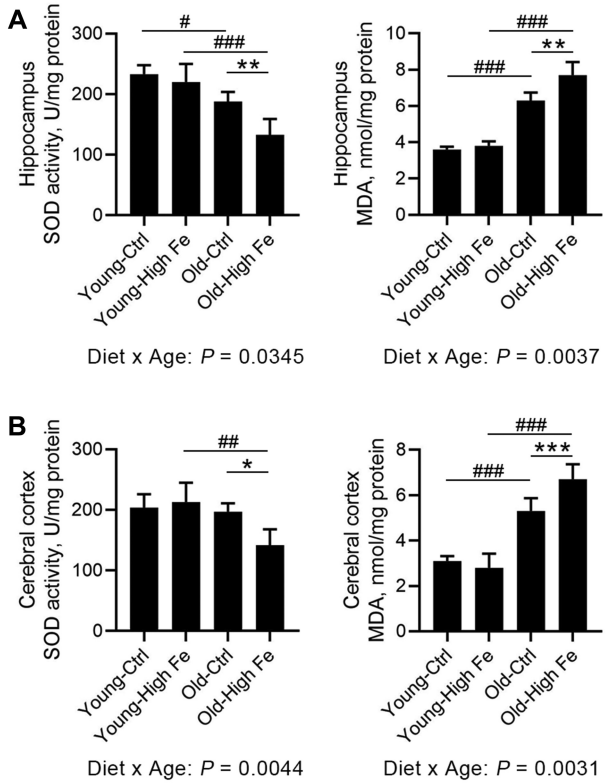

FIGURE 5 SOD activity and MDA concentration in the hippocampus (A) and cerebral cortex (B) of male C57BL/6J mice fed control or high iron diet for 7 mo beginning at 1 mo or 13 mo of age. Values are means ± SDs, $n = 6$. The P value of the interaction is presented when it reaches significance, and further analysis of diet simple effects and age simple effects was then performed. $^{*}P < 0.05$, $^{**}P < 0.01$, $^{***}P < 0.001$, different due to diet; $^{\#}P < 0.05$, $^{\#\#}P < 0.01$, $^{\#\#\#}P < 0.001$, different due to age. MDA, malondialdehyde; SOD, superoxide dismutase.

mice ($P < 0.001$) and Old-Ctrl mice ($P < 0.01$), consistent with enhanced oxidative stress. In addition, Old-Ctrl mice showed significantly lower SOD activity ($P < 0.05$) and greater MDA concentration ($P < 0.001$) than Young-Ctrl mice. The pattern of SOD activity and MDA concentration changes in cerebral cortex was similar to hippocampus, except that there was no significant difference in SOD activity between Old-Ctrl mice and Young-Ctrl mice (Figure 5B).

Old-High Fe mice display deficits of spatial learning and memory

The spatial learning and memory function of the 4 groups of mice was tested when the animals were 7 and 19 mo old. The swimming velocity of mice was significantly decreased by age ($P < 0.0001$), whereas there was no significant main effect of diet (**Figure 6**A). After 4 d of training, interactions between dietary iron and age were observed in platform crossings ($P = 0.0264$) and time spent in the target quadrant ($P = 0.0451$). Old-High Fe mice crossed the center of the target quadrant fewer times ($P < 0.05$) and spent less time in that quadrant ($P < 0.01$) than Young-High Fe mice and Old-Ctrl mice, suggesting deficits of spatial learning and memory (Figure 6B and C). However, a high iron diet had no significant effect on the behavior of the young age group, which is consistent with our previous work (14). During the 5-d experiment, all mice developed their ability to find the hidden platform, but a longer escape latency was induced by both iron treatment ($P = 0.0192$) and age ($P < 0.0001$) (Figure 6D).

Discussion

This study is a follow-up of our previous work (14), which has been briefly explained in the introduction section. Consistent with our previous report, feeding the male mice a high iron diet (~14 g Fe/kg) for 7 mo resulted in a significant lower body weight and higher iron concentrations in plasma and liver, and these effects were comparable between the 2 age groups. In contrast, brain iron concentration was only significantly affected by iron treatment when the mice were at an older age. This probably reflects an increase of the BBB permeability during aging (20, 21). Under physiologic conditions, iron transport across the BBB is mediated by the transferrin and transferrin receptor system (22). However, a recent study revealed an age-related shift in BBB transport from ligand-specific receptor-mediated transcytosis to ligand-nonspecific caveolar transcytosis (23), through which the plasma iron could easily enter the CNS. This concept may help to explain why the CNS becomes more sensitive to the elevation of systemic iron concentration at an old age.

Consistent with our previous report (14), although Young-High Fe mice did not show higher brain iron concentrations, their ferritin expression in hippocampus and cerebral cortex was significantly greater than in Young-Ctrl mice, suggesting a disrupted brain iron homeostasis despite the protection of the BBB. Furthermore, the high iron diet also induced the protein expression of p-tau and Aβ_{1-42} in hippocampus and Aβ_{1-42} in cerebral cortex, irrespective of the age of mice. Interestingly, the Aβ deposits in Young-High Fe mice were punctuate, similar to that in Old-Ctrl mice, whereas the Aβ deposits in Old-High Fe mice were plaque-like, mimicking the features of APP/PS1 mice as we previously reported (14). These results clearly demonstrated the bona fide contributions of dietary iron to the generation of AD biomarkers (24, 25).

Iron overload is usually accompanied by oxidative damage. Consistent with this, Old-High Fe mice showed oxidative stress in both hippocampus and cerebral cortex, paralleled by cognitive impairment. In contrast, mice at a younger age appeared to be relatively invulnerable to the high iron diet, as indicated by the unchanged SOD and MDA concentration in hippocampus and cerebral cortex as well as the behavioral test. These results suggest that iron entering the CNS may be highly detrimental. This viewpoint is supported by a recent study showing that 10-wk-old mice fed a lipophilic iron diet, which was assumed to penetrate the BBB, for 12 mo displayed significantly increased iron concentration and oxidative stress in brain regions, paralleled by spatial memory impairment (26). Indeed, dietary carbonyl iron supplementation usually did not induce significant brain iron accumulation and damage in adult animals; instead, hepatic iron overload and lipid peroxidation were widely acknowledged (14, 27–29). Only at an extremely high concentration (e.g., 20 g/kg) was dietary carbonyl iron found to be toxic to the brain, but in this case, the brain iron concentration was also increased, suggesting BBB impairment (30). To sum up, these studies suggest that dietary iron usually did not enter the CNS and thus was relatively safe to young adult animals. Nevertheless, as the BBB breaks down during aging, systemic iron might easily enter the CNS and induce oxidative damage, thereby causing cognitive dysfunction.

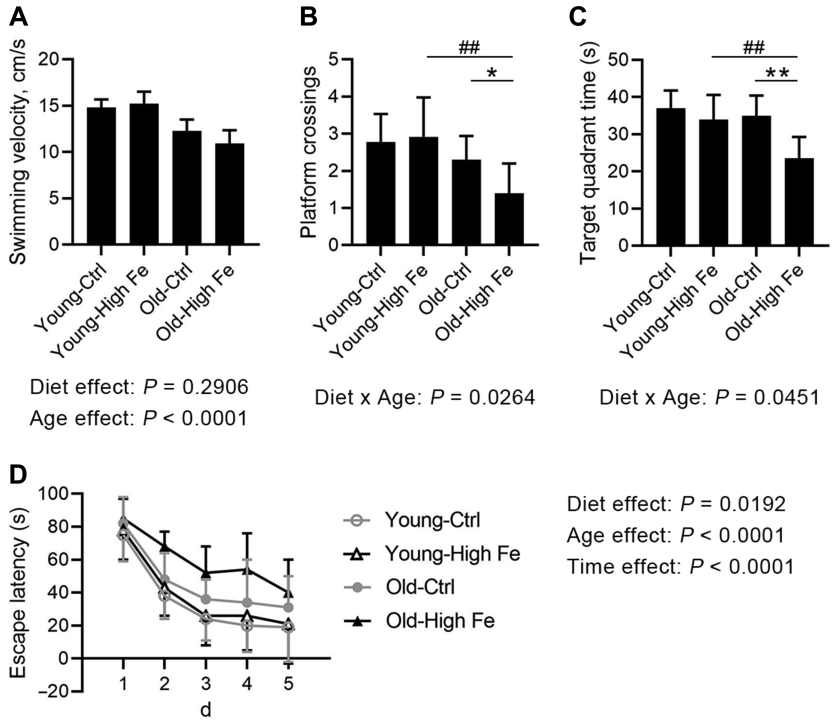

FIGURE 6 Swimming velocity (A), platform crossings (B), and time spent in the target quadrant (C) were recorded on day 5, the day a probe test was conducted, and escape latency (D) was recorded from days 1 to 5 in male C57BL/6J mice fed control or high iron diet for 6 mo beginning at 1 mo or 13 mo of age. Values are means ± SDs, $n = 8$. The P value of the interaction is presented when it reaches significance, and further analysis of diet simple effects and age simple effects was then performed. $^{*}P < 0.05$, $^{**}P < 0.01$, different due to diet; $^{\#\#}P < 0.01$, different due to age.

In conclusion, our work provides a comprehensive comparison on the impact of dietary iron overload on young and old male mice. Although AD pathologic markers were induced by iron treatment irrespective of the age of mice, only the old mice exhibited brain iron accumulation, oxidative stress, and learning and memory defects after the iron treatment. However, compared with our previous work (14), a limitation of this study is that only male mice were used. Considering that women are at higher risk of developing AD than men (31), future studies should include female mice. In addition, it should be noted that the dose of iron used in the iron-loaded diet is 200-fold greater than that of the control diet, and humans could by no means be supplemented with iron of such a high dose (14). Nevertheless, the etiology of human AD is very complicated, which may involve genetic background and various environmental stress conditions. As such, this study suggested that iron supplements might contribute to AD induction, especially for older people whose BBB function is getting worse.

Acknowledgments

The authors' responsibilities were as follows—HC: designed the research, analyzed the data, wrote and edited the manuscript; MC and JZ: performed the experiments, analyzed the data, prepared the figures, and wrote the manuscript; EX, CZ, and WZ: performed the experiments; and all authors: read and approved the final manuscript.

References

1. Rouault TA. Iron metabolism in the CNS: implications for neurodegenerative diseases. Nat Rev Neurosci 2013;14(8):551–64.
2. Anderson GJ. Mechanisms of iron loading and toxicity. Am J Hematol 2007;82(Suppl 12):1128–31.
3. Goodman L. Alzheimer's disease; a clinico-pathologic analysis of twenty-three cases with a theory on pathogenesis. J Nerv Ment Dis 1953;118(2):97–130.
4. Zhu WZ, Zhong WD, Wang W, Zhan CJ, Wang CY, Qi JP, Wang JZ, Lei T. Quantitative MR phase-corrected imaging to investigate increased brain iron deposition of patients with Alzheimer disease. Radiology 2009;253(2):497–504.
5. Connor JR, Snyder BS, Beard JL, Fine RE, Mufson EJ. Regional distribution of iron and iron-regulatory proteins in the brain in aging and Alzheimer's disease. J Neurosci Res 1992;31(2):327–35.
6. Collingwood JF, Mikhaylova A, Davidson M, Batich C, Streit WJ, Terry J, Dobson J. In situ characterization and mapping of iron compounds in Alzheimer's disease tissue. J Alzheimers Dis 2005 Aug;7(4):267–72.
7. Damulina A, Pirpamer L, Soellradl M, Sackl M, Tinauer C, Hofer E, Enzinger C, Gesierich B, Duering M, Ropele S, et al. Cross-sectional and longitudinal assessment of brain iron level in Alzheimer disease using 3-T MRI. Radiology 2020;296(3):619–26.
8. Mandel S, Amit T, Bar-Am O, Youdim MB. Iron dysregulation in Alzheimer's disease: multimodal brain permeable iron chelating drugs, possessing neuroprotective-neurorescue and amyloid precursor protein-processing regulatory activities as therapeutic agents. Prog Neurobiol 2007;82(6):348–60.
9. Leskovjan AC, Kretlow A, Lanzirotti A, Barrea R, Vogt S, Miller LM. Increased brain iron coincides with early plaque formation in a mouse model of Alzheimer's disease. Neuroimage 2011;55(1):32–38.
10. Rao SS, Lago L, Gonzalez de Vega R, Bray L, Hare DJ, Clases D, Doble PA, Adlard PA. Characterising the spatial and temporal brain metal profile in a mouse model of tauopathy. Metallomics 2020;12(2):301–13.
11. Rao SS, Adlard PA. Untangling tau and iron: exploring the interaction between iron and tau in neurodegeneration. Front Mol Neurosc 2018;11:276.
12. Ayton S, Fazlollahi A, Bourgeat P, Raniga P, Ng A, Lim YY, Diouf I, Farquharson S, Fripp J, Ames D, et al. Cerebral quantitative susceptibility mapping predicts amyloid-beta-related cognitive decline. Brain 2017;140(8):2112–19.
13. Zheng J, Jiang R, Chen M, Maimaitiming Z, Wang J, Anderson GJ, Vulpe CD, Dunaief JL, Chen H. Multi-copper ferroxidase-deficient mice

have increased brain iron concentrations and learning and memory deficits. J Nutr 2018;148(4):643–9.
14. Chen M, Zheng J, Liu G, Zeng C, Xu E, Zhu W, Anderson GJ, Chen H. High dietary iron disrupts iron homeostasis and induces amyloid-beta and phospho-tau expression in the hippocampus of adult wild-type and APP/PS1 transgenic mice. J Nutr 2019;149(12):2247–54.
15. Flurkey K, Currer JM, Harrison D. Mouse models in aging research. In: Fox JG, Davisson MT, Quimby FW, Barthold SW, Newcomer CE, Smith AL, editors. The mouse in biomedical research. 2nd ed. Burlington (VT): Academic Press; 2007. p. 637–72.
16. Reeves PG, Nielsen FH, Fahey GC, Jr. AIN-93 purified diets for laboratory rodents: final report of the American Institute of Nutrition ad hoc writing committee on the reformulation of the AIN-76A rodent diet. J Nutr 1993;123(11):1939–51.
17. Chen H, Su T, Attieh ZK, Fox TC, McKie AT, Anderson GJ, Vulpe CD. Systemic regulation of hephaestin and Ireg1 revealed in studies of genetic and nutritional iron deficiency. Blood 2003;102(5):1893–9.
18. Fuqua BK, Lu Y, Darshan D, Frazer DM, Wilkins SJ, Wolkow N, Bell AG, Hsu J, Yu CC, Chen H, et al. The multicopper ferroxidase hephaestin enhances intestinal iron absorption in mice. PLoS One 2014;9(6):e98792.
19. Konopka W, Kiryk A, Novak M, Herwerth M, Parkitna JR, Wawrzyniak M, Kowarsch A, Michaluk P, Dzwonek J, Arnsperger T, et al. MicroRNA loss enhances learning and memory in mice. J Neurosci 2010;30(44):14835–42.
20. Farrall AJ, Wardlaw JM. Blood-brain barrier: ageing and microvascular disease—systematic review and meta-analysis. Neurobiol Aging 2009;30(3):337–52.
21. Verheggen ICM, de Jong JJA, van Boxtel MPJ, Gronenschild E, Palm WM, Postma AA, Jansen JFA, Verhey FRJ, Backes WH. Increase in blood-brain barrier leakage in healthy, older adults. Geroscience 2020;42(4):1183–93.
22. Moos T, Morgan EH. Transferrin and transferrin receptor function in brain barrier systems. Cell Mol Neurobiol 2000;20(1):77–95.
23. Yang AC, Stevens MY, Chen MB, Lee DP, Stahli D, Gate D, Contrepois K, Chen W, Iram T, Zhang L, et al. Physiological blood-brain transport is impaired with age by a shift in transcytosis. Nature 2020;583(7816):425–30.
24. Guo C, Wang P, Zhong ML, Wang T, Huang XS, Li JY, Wang ZY. Deferoxamine inhibits iron induced hippocampal tau phosphorylation in the Alzheimer transgenic mouse brain. Neurochem Int 2013;62(2):165–72.
25. Sripetchwandee J, Wongjaikam S, Krintratun W, Chattipakorn N, Chattipakorn SC. A combination of an iron chelator with an antioxidant effectively diminishes the dendritic loss, tau-hyperphosphorylation, amyloids-beta accumulation and brain mitochondrial dynamic disruption in rats with chronic iron-overload. Neuroscience 2016;332:191–202.
26. Peters DG, Purnell CJ, Haaf MP, Yang QX, Connor JR, Meadowcroft MD. Dietary lipophilic iron accelerates regional brain iron-load in C57BL6 mice. Brain Structure Function 2018;223(3):1519–36.
27. Bacon BR, Tavill AS, Brittenham GM, Park CH, Recknagel RO. Hepatic lipid peroxidation in vivo in rats with chronic iron overload. J Clin Invest 1983;71(3):429–39.
28. Houglum K, Filip M, Witztum JL, Chojkier M. Malondialdehyde and 4-hydroxynonenal protein adducts in plasma and liver of rats with iron overload. J Clin Invest 1990;86(6):1991–8.
29. Kozlov AV, Bini A, Gallesi D, Giovannini F, Iannone A, Masini A, Meletti E, Tomasi A. 'Free' iron, as detected by electron paramagnetic resonance spectroscopy, increases unequally in different tissues during dietary iron overload in the rat. Biometals 1996;9(1):98–103.
30. Sobotka TJ, Whittaker P, Sobotka JM, Brodie RE, Quander DY, Robl M, Bryant M, Barton CN. Neurobehavioral dysfunctions associated with dietary iron overload. Physiol Behav 1996;59(2):213–19.
31. Gao S, Hendrie HC, Hall KS, Hui S. The relationships between age, sex, and the incidence of dementia and Alzheimer disease: a meta-analysis. Arch Gen Psychiatry 1998;55(9):809–15.